Articles

Effects of Temperature on Protein Structure and Dynamics: X-ray Crystallographic Studies of the Protein Ribonuclease-A at Nine Different Temperatures from 98 to 320 K[†,‡]

Robert F. Tilton, Jr.*
Miles Research Center, Miles Inc., 400 Morgan Lane, West Haven, Connecticut 06516
John C. Dewan
Department of Chemistry, New York University, New York, New York 10003-6603
Gregory A. Petsko
Rosenstiel Basic Medical Sciences Research Center, Brandeis University, Waltham, Massachusetts 02254-9110
Received January 15, 1991; Revised Manuscript Received December 18, 1991

ABSTRACT: Structures using X-ray diffraction data collected to 1.5-Å resolution have been determined for the protein ribonuclease-A at nine different temperatures ranging from 98 to 320 K. It is determined that the protein molecule expands slightly (0.4% per 100 K) with increasing temperature and that this expansion is linear. The expansion is due primarily to subtle repacking of the molecule, with exposed and mobile loop regions exhibiting the largest movements. Individual atomic Debye–Waller factors exhibit predominantly biphasic behavior, with a small positive slope at low temperatures and a larger positive slope at higher temperatures. The break in this curve occurs at a characteristic temperature of 180–200 K, perhaps indicative of fundamental changes in the dynamical structure of the surrounding protein solvent. The distribution of protein Debye–Waller factors is observed to broaden as well as shift to higher values as the temperature is increased.

Temperature controls the average structural and dynamical properties of molecules. X-ray crystallography provides a powerful technique to obtain high-resolution models of the average molecular structure and to examine the spatial distribution of atomic motions. High-resolution X-ray crystallography carried out as a function of temperature allows one, in principle, to explore the physical–chemical nature of molecular topography and to probe the subtle balance of bonded and nonbonded forces that stabilize structure and control dynamics.

Multiple-temperature crystallography has been used recently to study the effects of temperature on the structure and dynamics of the all α-helical protein myoglobin from sperm whale (Frauenfelder et al., 1979, 1987; Hartmann et al., 1982). Analysis of two structures determined with data collected at 80 and 300 K indicates that an increasing temperature results in an anisotropic expansion of 2–3% in protein volume with a nonuniform increase in atomic motions as measured by individual Debye–Waller factors. Analysis of the expansion revealed that surface loops are involved and that the volume increase is distributed into subatomic-sized spaces rather than larger water-sized cavity spaces. The larger Debye–Waller factors at 300 K were attributed to the increased magnitude of vibrational motions and the increased distribution of conformational microstates. Structures of myoglobin at several intermediate temperatures have also been investigated (Parak et al., 1987). Because myoglobin is composed entirely of α-helices packed around a large, planar prosthetic group, we have undertaken a study to explore the structure and dynamics of a protein that has no cofactor and is primarily β-sheet. We have chosen for this purpose the protein bovine pancreatic ribonuclease-A.

Ribonuclease-A, a small monomeric enzyme of molecular weight 13 683 (124 amino acids) is a kidney-shaped molecule consisting of an N-terminal α-helix and two shorter helices packed against a central, twisted antiparallel β-sheet (Figure 1). The approximate dimensions of the molecule are 37 by 45 by 34 Å, and the protein fold is stabilized internally by four disulfide bridges. The function of the enzyme is to hydrolyze single-stranded RNA molecules by cleaving the phophodiester linkage, leaving terminal 3′-pyrimidine nucleotide monophosphates. The RNA substrate binds in the deep cleft of the kidney-shaped enzyme. In terms of the relationship between structure and function, mechanisms of protein folding, and the physical–chemical properties of a protein molecule, ribonuclease-A is one of the most thoroughly studied of all enzymes. The first three-dimensional structure of ribonuclease-A was reported in 1967 (Avey et al., 1967; Kartha et al., 1967). Since then, several different groups have extended the resolution (Borkakoti et al., 1982, 1984; Svensson et al., 1986; Wlodawer et al., 1988), studied structural aspects of the enzyme mechanism (Borkakoti, 1983; McPherson et al., 1986; Campbell & Petsko, 1987), and explored questions of protein hydration by both X-ray and neutron crystallography (Wlodawer & Sjolin, 1983; Wlodawer et al., 1986).

Ribonuclease-A is an ideal candidate for low-temperature physical–chemical studies by X-ray diffraction. It is a relatively small and compact protein and forms large, well-ordered crystals in aqueous–organic solvents that diffract to very high resolution. Early work indicated that crystals of ribonuclease-A could be cooled to 120 K without deleterious effects

[†] This work was supported by grants from the NIH (F32 AM07339 and GM38758).
[‡] The coordinates for the nine ribonuclease-A structures have been submitted to the Brookhaven Protein Data Bank under the names 1-9RAT.

0006-2960/92/0431-2469$03.00/0 © 1992 American Chemical Society

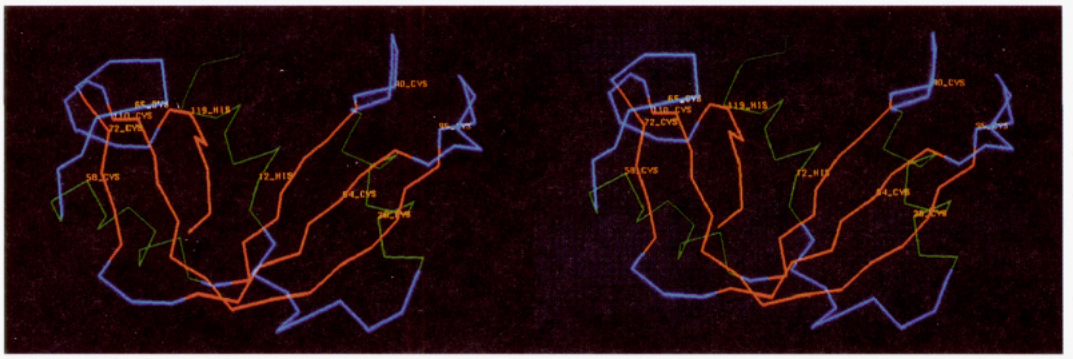

FIGURE 1: Model of ribonuclease-A, in stereo, color coded for elements of secondary structure. The protein is kidney shaped with a long N-terminal α-helix and two shorter α-helices (green) packed against the central, twisted β-pleated sheet (red) and large solvent-exposed loops (blue) that are stabilized by the four disulfide bridges (26–84; 40–95; 58–110; 65–72). The active site cleft of ribonuclease-A is flanked by two histidine residues (His 12 and His 119).

Table I: Data Collection and Crystal Preparation

temp (K)	resolution (Å)	data collection	instrument	mount	mother liquor	data collection times (days)
98	1.5	background–peak–background	Enraf Nonius CAD4	glass fiber	50% MPD	14
130	1.5	background–peak–background	Enraf Nonius CAD4	glass fiber	50% MPD	14
160	1.5	background–peak–background	Enraf Nonius CAD4	capillary	50% MPD	14
180	1.5	background–peak–background	Enraf Nonius CAD4	glass fiber	50% MPD	14
220	1.5	background–peak–background	Enraf Nonius CAD4	glass fiber	50% MPD	10
240	1.5	background–peak–background	Nicolet P3-LT1	capillary	50% MeOH	14
260	1.5	background–peak–background	Nicolet P3-LT1	capillary	50% MeOH	14
300	1.5	background–peak–background	Nicolet P3-LT1	capillary	50% MeOH	10
320	1.5	Wyckoff peak	Nicolet P3-LT1	capillary	50% MeOH	5

(Petsko, 1975). We present in this paper detailed comparisons of nine X-ray structures of ribonuclease-A refined with 1.5-Å data collected at temperatures ranging from 98 to 320 K. In this first paper we attempt only to explore the overall effects of temperature on the structure and dynamics of the protein molecule itself. Future analysis will examine the protein–solvent interface in an attempt to understand the effects of temperature on the hydrogen-bonded network that encompasses the protein molecule.

Experimental Procedures

The wide range of temperature explored in this study necessitated different crystal mother liquors, crystal mounting techniques, data collection instruments, temperature controllers, and data collection procedures. The common elements for all of the data collects were as follows: (1) Bovine pancreatic ribonuclease-A, type III, was obtained from Sigma Chemical Co. and used without further purification. (2) Crystals were grown at 20 °C from unbuffered solutions of 12 mg/mL protein in 50% (v/v) methanol–water adjusted to pH* 5.5 with sodium hydroxide (Gilbert et al., 1982; Campbell & Petsko, 1987). pH* indicates the proton activity of the aqueous–organic solution at the given temperature (Douzou, 1977). (3) Crystals for data collection were typically 1.0 × 0.7 × 0.7 mm in size. (4) Unique data were collected to a nominal resolution of 1.5 Å (18 500 reflections). (5) Data were collected by single-counter diffractometry using Ni-filtered Cu Kα radiation of wavelength 1.5418 Å from sealed-tube sources (30 mA, 40 kV). (6) A single crystal was used for each data set at a given temperature. This obviated the need to scale data together from multiple crystals at any individual temperature.

Crystal Preparation and Data Collection. Specifics of the crystal mounting and data collection at each of the nine individual temperatures are summarized in Table I. Low-temperature data sets (temperatures less than 220 K) were collected from crystals in which 2-methyl-2,4-pentanediol (MPD) was substituted for methanol as the cryoprotective mother liquor. MPD is chosen for its ability to supercool rather than freeze at volume fractions greater than 50% (v/v) and temperatures less than 220 K. Crystals grown originally from 50% (v/v) methanol–water were transferred into 50% (v/v) MPD–water, pH* 5.5 at a temperature of 277 K. The transfer was done slowly to minimize "dielectric" shock and crystal cracking. Data were collected on two different diffractometers: a Nicolet P3 with an LT1 coaxial gas-flow constant-temperature device and an Enraf Nonius CAD4 with an Enraf Nonius fixed vertical gas-flow constant-temperature device. While the CAD4 system is capable of lower temperature (100 K), the fixed gas cooling stream can create problems that require specialized crystal mounting techniques. The Nicolet coaxial gas stream, on the other hand, minimizes the problem of gas turbulence but is more difficult to use efficiently below 180 K. Both temperature control systems are stable during data collection to ±2 °C. Crystal mounting techniques were dictated by the temperature control system. Higher temperatures require that crystals be mounted conventionally in capillaries to prevent loss of the volatile organic solvent in the normal crystal mother liquor. However, with low temperatures and the fixed gas stream arrangement of the CAD4, crystals mounted in capillaries cause problems due to cooling gas turbulence and frost buildup; hence, for nearly all of the low-temperature data sets, crystals were affixed directly to glass fibers with uncured epoxy cement and rapidly cooled (Dewan & Tilton, 1987). Crystals mounted in this manner display virtually no radiation damage but do exhibit a slight increase in mosaic spread (scan half-width of 0.3°) (Young et al., 1990). This crystal mounting method was first reported by Hass and Rossmann in 1973 and is used routinely in small-molecule crystallography for air- or moisture-sensitive crystals (Huffman et al., 1973; Hope & Power, 1983; Listemann et al., 1985; Schumann et al., 1986; Pederson et al., 1987). Two other groups have coadapted the glass fiber mounting technique for work with macromolecules (Hope,

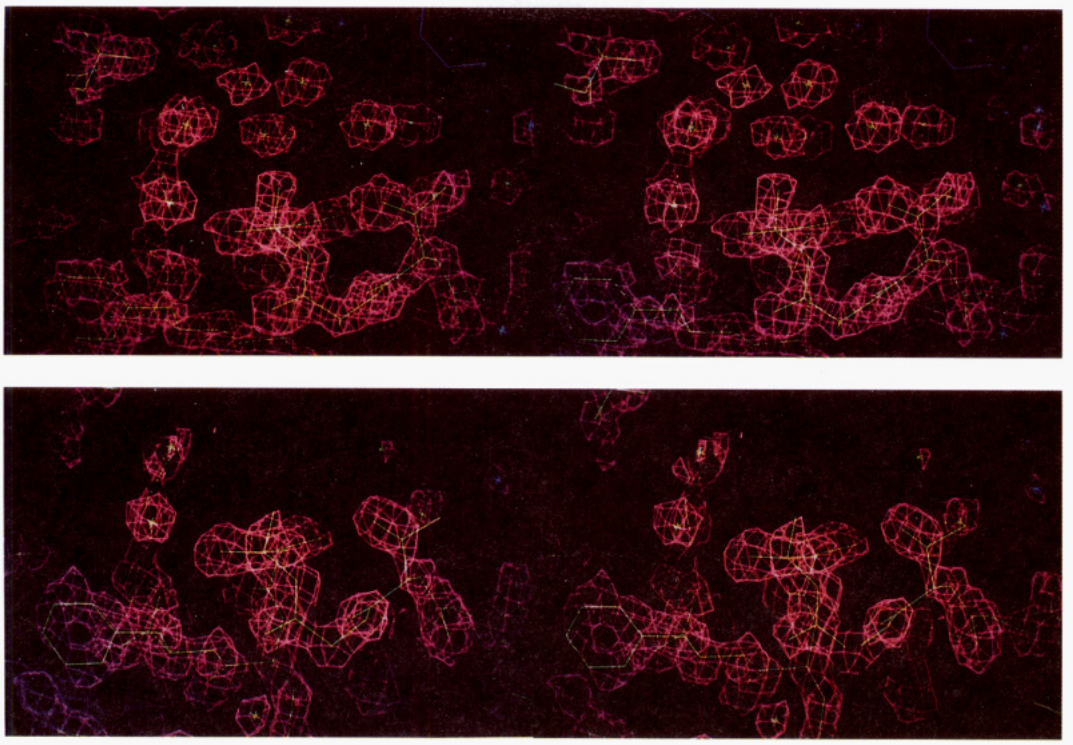

FIGURE 2: Representative electron density ($2F_o - F_c$) map at the protein surface at 98 K (a, top) and 320 K (b, bottom). Density is shown in purple and is contoured at 1.5σ. Symmetry-related molecules are shown in blue. The quality of the maps is improved significantly at reduced temperature with a large increase in the number of discrete surface waters.

1988; Hope et al., 1989; Muchmore & Watenpaugh, 1988). A review of macromolecular crystallography at low temperature has appeared recently (Hope, 1990).

Most of the data collections used conventional background–peak–background full-width ω scans with 50% of the total scan time spent on individual backgrounds. Scan widths were typically 0.7–1.0° on ω. The total time spent on each reflection was 60 s, and the total time spent per data set was typically 14 days. A minimum of three reflections distributed evenly in reciprocal space were collected every 200–400 data reflections to monitor crystal movement and radiation decay. The highest temperature data set (320 K) was collected with peak scans using backgrounds corrected by an empirical background correction curve (Wyckoff et al., 1967). Peak scans were necessitated by elevated radiation-induced decay at this temperature. Use of the limited peak scan procedure reduced the data collection time from 14 to 5 days. Data sets at temperatures of 240, 260, and 320 K were already present in the laboratory and were kindly provided by Dr. Stephen K. Burley and Dr. William A. Gilbert.

Data Reduction and Model Refinement. Original data sets at the nine different temperatures were corrected for background, absorption (North et al., 1968), Lorentz and polarization factors, and, when necessary, radiation-induced decay. Below temperatures of 220 K, ribonuclease-A crystals mounted on glass fibers exhibit virtually no radiation decay. At higher temperatures a linear decay of up to 30% was observed. These reduced data sets were refined against an earlier model of the structure of ribonuclease-A at room temperature by the method of restrained least-squares refinement using the program PROLSQ (Konnert & Hendrickson, 1980). The refinements of data sets at the different temperatures used identical geometrical and temperature factor weighting schemes. The initial models did not include solvent molecules or counterions. All of the refinements were started with a single overall Debye–Waller factor that was set initially to be proportional with temperature to the average Debye–Waller value from an earlier refined model of ribonuclease-A (260 K). Data between 10.0- and 3.0-Å resolution were used initially with data from higher resolution shells added gradually until all of the data with intensities greater than twice their standard deviation were included. The number of reflections included in the different refinements ranged generally between 60% and 80% of the total number expected in a unique data set to 1.5-Å resolution. After refinement with uniform Debye–Waller factors, solvent molecules and counterions were identified using $3F_o - 2F_c$, $2F_o - F_c$, and $F_o - F_c$ Fourier syntheses in which questionable regions of the structure were deleted from the calculation of the F_c and phases. Electron density maps were displayed with the program FRODO (Jones, 1982) on an Evans and Sutherland PS390 molecular graphics system (Figure 2). Refinement was then continued using individual isotropic Debye–Waller factors for all atoms. Refinement and manual adjustment of side-chain and solvent positions was iterated until the R factor converged and no interpretable features were present in the difference electron density maps. Alternate conformations of some side-chain positions were noted but were not included in the refinement. A summary of the unit cell dimensions, data collection statistics, refinement parameters, and current R factors is listed in Table II. Analysis of these structures was begun only after all of the individual refinements of the nine structures were completed.

RESULTS

Analysis of these multiple-temperature X-ray crystallographic structures is divided into two parts. Part 1 focuses on the effects of temperature on the average structure of the protein molecule and changes of the protein packing within the crystalline lattice. Part 2 examines the effects of temperature on protein dynamics as reflected in the behavior of the individual protein atomic Debye–Waller factors.

Structure. Crystals of ribonuclease-A used in these experiments belong to the space group $P2_1$ with a single protein molecule in each asymmetric unit. Unit cell parameters de-

Table II: Statistics

	Data Collection				
	unit cell constants (Å)				
temp (K)	*a*	*b*	*c*	β-angle (deg)	no. of reflections [$>2\sigma(I)$]
98	29.48	38.08	52.97	106.09	11214
130	29.48	38.12	53.24	106.10	12649
160	29.51	38.08	52.93	106.32	15873
180	29.52	38.18	53.21	106.15	14646
220	30.14	38.23	53.16	106.96	10235
240	30.15	38.22	53.02	106.45	14779
260	30.16	38.18	53.14	106.40	11441
300	30.27	38.43	53.79	107.09	14310
320	30.40	38.30	53.30	106.90	12373

	Structure Refinement								
temp (K)	SD1	SD2	SD3	SP	SC	ST2	ST3	ST4	*R* factor (%)
98	0.024	0.034	0.045	0.016	0.139	3.3	13.7	16.7	17.1
130	0.024	0.035	0.045	0.018	0.161	3.2	14.3	18.0	14.8
160	0.019	0.033	0.045	0.017	0.163	3.3	13.3	17.9	14.9
180	0.026	0.037	0.045	0.019	0.170	3.5	13.6	20.3	14.9
220	0.022	0.036	0.039	0.016	0.146	3.3	16.2	17.6	15.1
240	0.026	0.035	0.046	0.018	0.150	4.1	14.5	17.5	15.2
260	0.019	0.033	0.040	0.014	0.135	3.5	16.9	20.2	16.1
300	0.023	0.035	0.045	0.016	0.158	4.5	17.1	18.7	15.8
320	0.030	0.045	0.053	0.020	0.170	3.3	17.4	21.0	19.1
target	0.030	0.040	0.050	0.025	0.150	5	15	15	

[a] Mean estimated standard deviation (distances, Å; angles, deg): SD1, bond length (1–2 neighbor); SD 2, angle length (1–3 neighbor); SD3, intraplanar length (1–4 neighbor); SP, deviation from planarity; SC, chiral volume; ST2, torsion angle planar; ST3, torsion angle staggared; ST4, torsion angle transverse. *R* factor = $\sum(F_o - F_c)/\sum F_o$.

Table III: Root Mean Square Deviations[a]

	130 K	160 K	180 K	220 K	240 K	260 K	300 K	320 K
98 K	0.136	0.136	0.163	0.234	0.253	0.215	0.304	0.283
	(0.457)	(0.371)	(0.796)	(0.817)	(0.717)	(0.802)	(0.905)	(0.798)
130 K		0.145	0.093	0.264	0.361	0.230	0.227	0.283
		(0.427)	(0.801)	(0.825)	(0.776)	(0.784)	(0.894)	(0.791)
160 K			0.154	0.252	0.218	0.223	0.301	0.276
			(0.791)	(0.814)	(0.707)	(0.804)	(0.907)	(0.796)
180 K				0.271	0.249	0.234	0.275	0.279
				(0.817)	(0.629)	(0.766)	(0.909)	(0.670)
220 K					0.142	0.157	0.269	0.223
					(0.585)	(0.528)	(0.906)	(0.674)
240 K						0.127	0.245	0.187
						(0.501)	(0.797)	(0.366)
260 K							0.215	0.171
							(0.788)	(0.554)
300 K								0.172
								(0.811)

[a] The upper number is the rms for main-chain atoms. The lower number (in parentheses) is the rms for all atoms.

termined for crystals at the different temperatures indicate an overall expansion of the unit cell with increasing temperature. The increase is linear for the *a*, *b*, and *c* axes as well as the β-angle, with the largest absolute change occurring along the *a* axis (Table II). The overall change in the unit cell volume between the temperatures of 98 and 320 K is 4.7%, representing a change of 3340 Å^3.

This volume change can occur in two ways: (1) as a result of structural changes within individual protein molecules and in the surrounding solvent structure and (2) as a result of changes in the orientation or packing of molecules in the unit cell. Evidence exists that the observed unit cell changes arise from structural changes of both types.

Several analyses indicate subtle changes in the protein structure with temperature. While the effects are small, they are consistent. Root mean square (rms) deviations in atomic coordinates report on the global similarities between structures. These are presented in Table III as a matrix of rms deviations between all possible pairs of structures. Overall, the three-dimensional structure of ribonuclease-A does not undergo a large change over the temperature range 98–320 K. However, rms values computed for main-chain atoms (Cα, C, N) and for all atoms indicate that structures that are close together in temperature have smaller deviations in general than structures that are widely separated in temperature. The deviation for main-chain atoms varies between 0.1 and 0.3 Å, while the deviation for all atoms varies between 0.4 and 0.9 Å over the observed temperature range.

This structural deviation is manifested in global volume changes in the protein molecule as the temperature varies. Two indicators of volume, the radius of gyration (R_g) and the analytically determined probe-accessible volume (Connolly, 1985), indicate a slight expansion of the protein that is linear with increasing temperature (Figure 3). The percentage change in volume calculated from the probe-accessible surfaces is approximately 0.4% per 100 K. A 1% change in volume for ribonuclease-A would be 150 Å^3—equivalent to the volume of about five water molecules. This raises the question of whether volume changes of this magnitude produce atom-sized cavities in the protein. However, no atom-sized cavities, as defined by a probe sphere of 1.4-Å radius or larger, are observed in the ribonuclease-A molecule at any of the nine

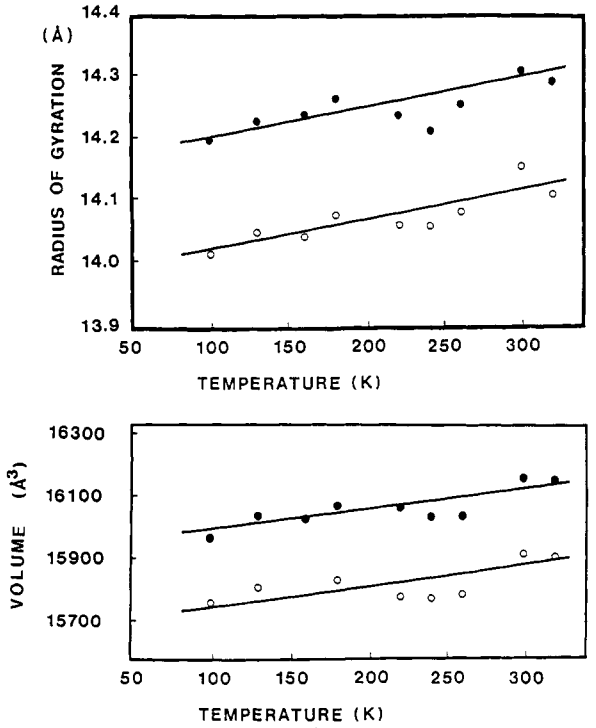

FIGURE 3: Radius of gyration (R_g) of ribonuclease-A calculated using all atoms (●) and main-chain atoms (○) as a function of temperature (top). Analytically determined probe-accessible volume (Connolly, 1985) of ribonuclease-A as a function of temperature using a 1.6-Å radius probe (●) and a 1.4-Å radius probe (○) (bottom).

temperatures. The volume increase arises primarily from movements of the extended loops of the protein and an increase in the subatomic-sized spaces within the molecule. Movements of the extended loops are reflected in changes in the number of long interatomic distances between the 98 and the 320 K structures. An examination of the difference in the number of interatomic distances between the structures at these two temperature extremes illustrates that the observed expansion occurs by reducing slightly the number of atomic distances in the range of 8–10 Å in favor of longer distances in the range of 14–20 Å (Figure 4). The atoms primarily responsible for this shift are in the protruding loops. Changes in the volume associated with the subatomic spaces can be indirectly examined by computing the number of short interatomic distances. A decrease in the number of these distances indicates an increase in the subatomic volume. Indeed, a 2.7% decrease of all interatomic distances less than 3.25 Å is observed as the temperature is increased from 100 to 300 K (an average of 2231 distances at 98 and 130 K and an average of 2170 distances at 300 and 320 K). Distances involving polar nitrogen and oxygen atoms decrease by 2.4% while distances involving nonpolar carbon and sulfur atoms decrease by 3.1%. Potential protein–protein hydrogen bonds, as monitored by distances less than 3.25 Å, involving only nitrogen and oxygen were found to decrease only marginally (1%) as the temperature is increased. It is believed that both larger motions of secondary structure, particularly exposed surface loops, and a decrease in local atomic packing density are responsible for the observed expansion of the protein molecule as the temperature is increased.

The linearity of both the radius of gyration and the overall probe-accessible volumes with temperature indicates that the change in mother-liquor solvent from MPD to methanol between 220 and 240 K has no apparent effect on the structure of ribonuclease-A. Other crystallographic studies of this enzyme in methanol, ethanol, 2-methyl-2-propanol, and MPD

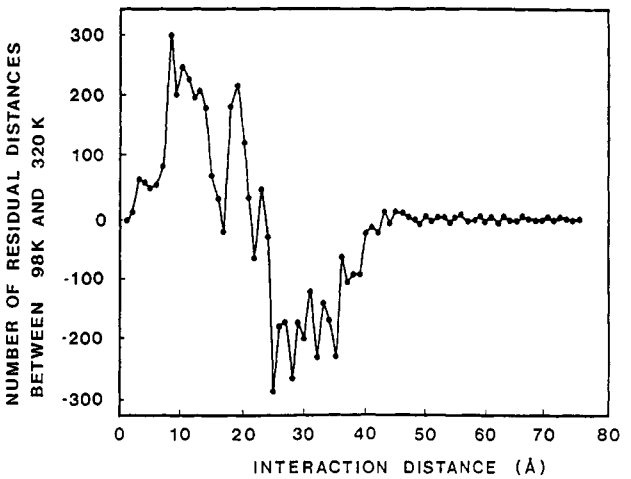

FIGURE 4: Difference in the number of interatomic distances calculated between ribonuclease-A at 98 and 320 K as a function of distance. A positive number indicates that the protein structure at 98 K has more atomic interactions at this distance while a negative number indicates that the protein structure at 320 K has more atomic interactions at this distance.

at room temperature have also revealed that the crystallographic unit cell is nearly insensitive to the specific organic crystallization solvent (King et al., 1956).

Volume and structural changes of the protein molecule can be followed in more detail by the use of difference distance matrices. Conventional distance matrices using the Cα atom positions are subtracted at two separate temperatures to give an unbiased view of regional perturbation, i.e., relative expansion and contraction within the protein molecule (Nishikawa et al., 1972). Random errors in comparing small differences are reduced by averaging structures close together in temperature (320 and 300 K, 220 and 180 K, 130 and 98 K). To reveal relative movements of secondary structure elements in the protein, the individual atom-pair difference distances are also summed and normalized over the residues defining elements of secondary structures, i.e., helices, strands, and turns. Difference distance matrices comparing these averaged structures are shown in Figure 5, with tabulated values over the various secondary structure elements given in Table IV. These results confirm that the protein expands anisotropically with increasing temperature and that the expansion is due primarily to movements of protruding protein loops (T1, T3, T5) and secondary structure α-helical elements (H2, H3), while the central β-sheet strands are the most rigid. Surface characteristics such as hydrophobic- and hydrophilic-exposed surface areas change only slightly with temperature. However, due to the intimate relationship between the protein molecule and the surrounding water structure, further analysis of the surface characteristics of ribonuclease-A at the different temperatures must await more complete analysis of the effects of temperature variation on the water environment.

In addition to the observed structural changes within the individual protein molecule, changes are also observed in contacts between protein molecules within the crystalline environment at different temperatures. In general, the number of amino acid residues involved in protein–protein contacts decreases slightly as the temperature is increased. Between the temperatures of 98 and 320 K, the number of short contacts less than 3.5 Å decrease by two while the number of longer contacts less than 4.5 Å decrease by ten. The total number of amino acids involved in protein contacts less than 4.5 Å is 46 at 98 K, 44 at 160 K, 43 at 220 K, 37 at 240 K, 36 at 300 K, and 36 at 320 K. The decrease in crystalline

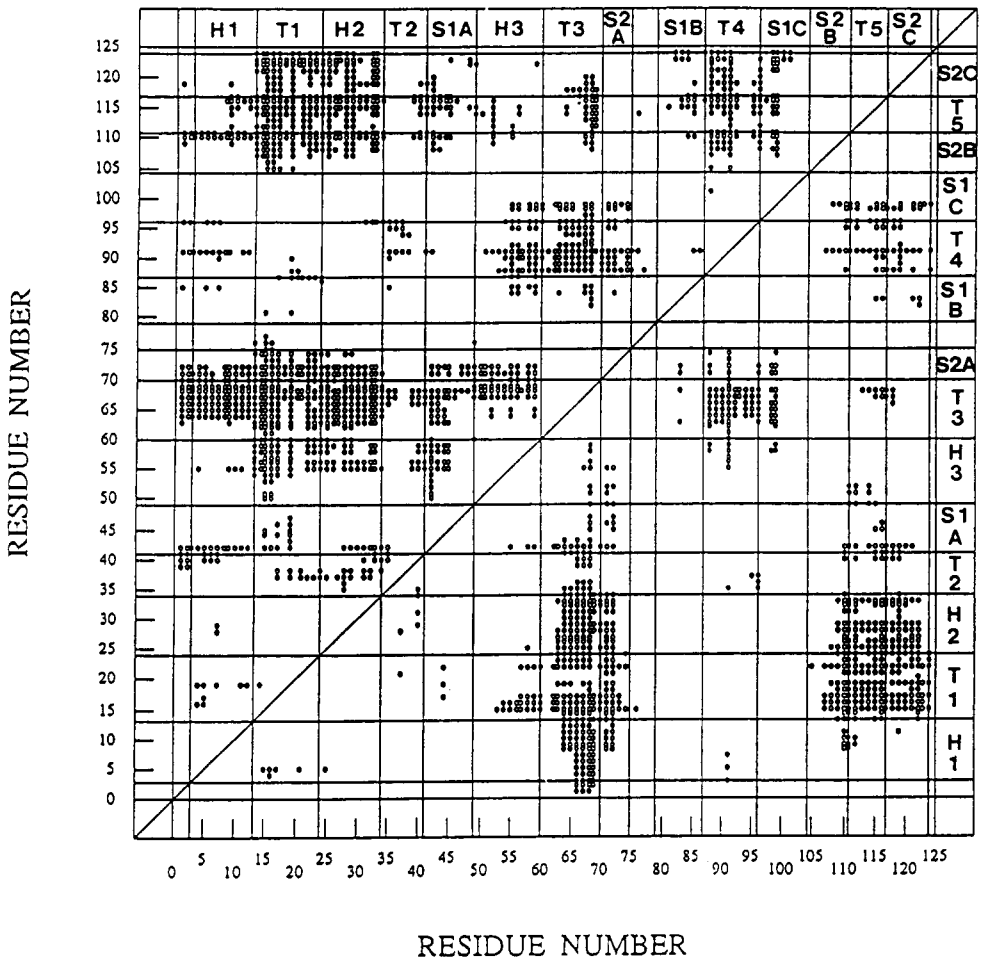

FIGURE 5: Difference distance maps of the Cα positions of ribonuclease-A at low temperature (average of 98 and 130 K), intermediate temperature (average of 180 and 220 K), and high temperature (300 and 320 K). Difference distances greater than +0.3 Å are denoted with a circle, and residue numbers and secondary structure elements are labeled. The upper-left portion illustrates the differential expansion as the temperature is increased from 100 to 300 K. The lower-right portion illustrates the differential expansion as the temperature is increased from 200 to 300 K. The expansion is due primarily to movements of the protruding loops. A quantitative summary of the difference distance map is given in Table IV.

contacts is observed both in regions of high-contact density and in isolated single residue–residue interactions. This decrease reflects the expansion of the unit cell as well as changes within the individual protein molecule (Figure 6). We caution, however, that protein–protein contacts are only one factor in the lattice environment and that we have not yet considered the role of bridging solvent molecules in our analysis.

Dynamics. Protein dynamics are observed in X-ray crystallography in two ways. Motion is observed implicitly in the electron density maps: alternate conformations or, more commonly, the absence of electron density for regions of the protein indicates positional disorder that may be static but which is often assumed to be dynamic. Evidence for motion may also be found explicitly in the isotropic atomic Debye–Waller parameter used in refinement to model the spread of electron density around the average position of each atom. The Debye–Waller parameter B (temperature factor) is related to the mean square displacement of an atom $\langle x \rangle^2$ ($B = 8\pi^2\langle x \rangle^2$) and thereby reflects uncertainty in the atomic position. Possible contributions to this uncertainty include errors in the model, static disorder within the crystalline lattice, unresolved conformations of the protein molecule, and dynamic disorder due to thermal motions. While the Debye–Waller factor is a difficult parameter to interpret unambiguously, we proceed with the understanding that it is related in large part to the dynamic behavior of protein atoms (Petsko & Ringe, 1984). Examination of the temperature dependence of this parameter can distinguish between predominantly static and dynamic disorder, since the former should be independent of temperature to a first approximation, while the latter can display significant and complex temperature dependence.

Refined Debye–Waller factors from these models of ribonuclease-A have been analyzed in several ways. The average Debye–Waller factor for all protein atoms at each temperature is shown in Figure 7. A biphasic curve is observed that can be approximated by a linear increase in slope of 1.2 Å^2 per 100 K from 100 to 200 K, followed by a second linear increase with a steeper slope of 6.4 Å^2 per 100 K from 200 to 320 K. Biphasic behavior cannot be attributed to the change in solvent from methanol to MPD since the solvent change occurs at a temperature 40 deg higher than the location of the break in slope, and the points from structures in MPD above the break are linear with those from methanol. Moreover, there is independent evidence from several studies that a change in the dynamic properties of many protein crystals and protein solutions occurs in the neighborhood of 200 K. Electron-transfer experiments between donor and acceptor protein molecules in solution exhibit a biphasic dependence of rate with temperature with the break in the curve near 200 K (Peterson-Kennedy et al., 1986). Calorimetry and infrared absorption studies on peptides and proteins indicate a sharp transition in the properties of the solvent around protein molecules that once again occurs around 200 K (Doster et al., 1986). Mössbauer (Keller & Debrunner, 1980; Parak et al., 1982; Bauminger

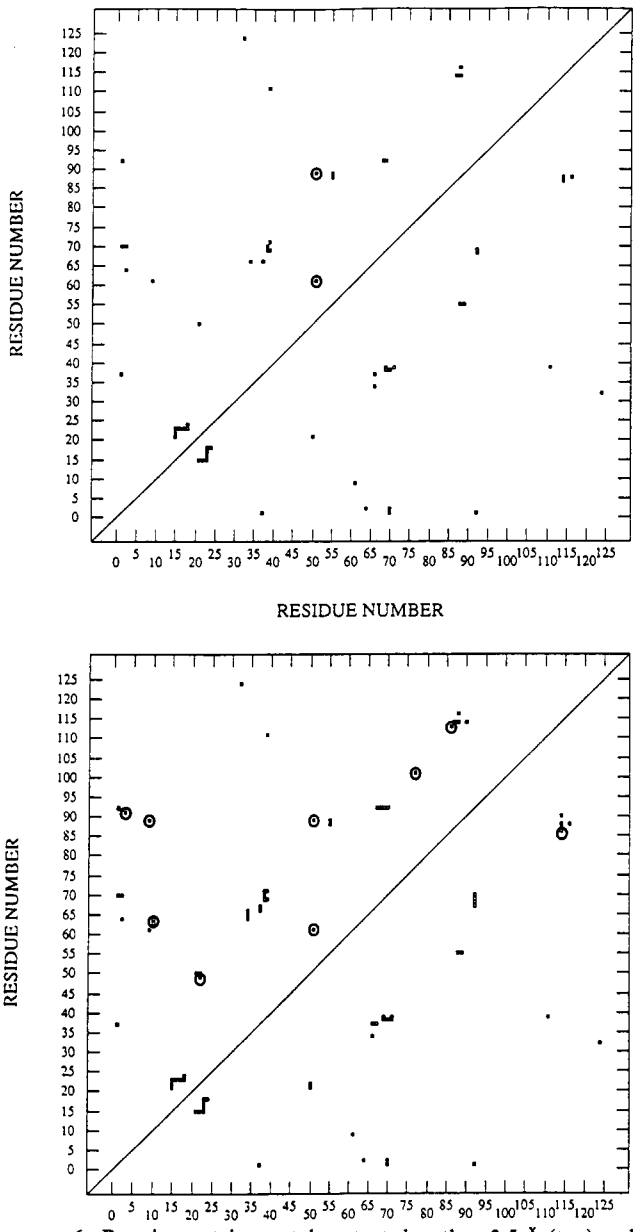

FIGURE 6: Protein–protein crystal contacts less than 3.5 Å (top) and less than 4.5 Å (bottom) for the 98 K molecule in the 98 K unit cell (upper left) and the 320 K molecule in the 320 K unit cell (lower right). Contacts that are different are circled.

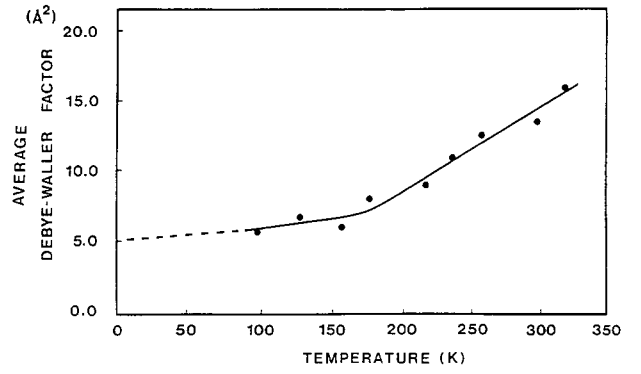

FIGURE 7: Average protein Debye–Waller factor as a function of temperature indicating biphasic behavior with a small positive slope of 1.2 Å²/100 K from 100 to 200 K and a larger positive slope of 6.4 Å²/100 K from 200 to 320 K.

et al., 1983), NMR (Usha & Wittebort, 1989), and inelastic neutron scattering studies (Doster et al., 1989; Cusack, 1989) indicate a change in the behavior of protein solution properties around the 200 K temperature. Finally, attempts to maintain a ribonuclease-A crystal at this transition temperature of 200 K for X-ray data collection were not successful as the crystal rapidly became opaque and ceased to diffract (Dewan & Tilton, 1987). It is believed that a characteristic change occurs primarily in the coordination shells of water that are bound to the surface of the protein. The strong coupling between the structure and dynamics of the solvent shell and the protein is believed responsible for the biphasic behavior observed for the protein atomic Debye–Waller factors. The crystalline structures of ribonuclease-A at low temperatures indicate that the first hydration shell contains nearly all water molecules. It is therefore assumed that the properties observed in this study depend primarily on the protein–water interface, rather than on the cryoprotectant that is used. The nonlinearity of the dynamic behaviors of ribonuclease-A (and many other proteins) with temperature is an important phenomenon that deserves further experimental and theoretical study. The work presented in a future paper will provide an atomic resolution view of the organization of bound solvent molecules on the surface of ribonuclease-A at all nine temperatures. Preliminary analysis indicates a large decrease in the number of ordered water molecules as the temperature is increased. For the present, we concentrate on the atoms of the protein itself.

The average Debye–Waller factor for all protein atoms increases from 6.6 Å² at 98 K to 15.7 Å² at 320 K—an increase of 138%. The average Debye–Waller factor at low temperatures (less than 180 K) is similar to that observed experimentally in many small organic molecules (Stout & Jensen, 1989). Histograms of the individual atomic Debye–Waller factors indicate that increasing temperature results not only in an increase in the overall Debye–Waller factor but also in a distinct broadening of the distribution (Figure 8). The more complicated distributions at the higher temperatures may reflect increasing anharmonicity in the atomic motions.

Plots of the average main-chain Debye–Waller factor as a function of protein residue are also shown for several temperatures (130, 180, 240, and 300 K) in Figure 9. These data illustrate an overall increase superimposed on a strong anisotropy in the temperature dependence of the Debye–Waller factor as the temperature increases. The overall changes are compelling evidence that the Debye–Waller factors for ribonuclease-A reflect predominantly intramolecular motion rather than static atomic or lattice disorder. Anisotropic temperature dependence implies that the forces that stabilize structure and govern dynamics are not uniform throughout the protein.

Some indication of how these forces vary can be obtained by plotting the Debye–Waller factor for an individual atom or residue as a function of temperature. The data obtained in this study allow such plots, in principle, to be made for every one of the almost 1000 non-hydrogen atoms in ribonuclease-A. Such plots proved to be relatively noisy, but qualitative information can be obtained by averaging the atomic values for only the main-chain atoms in a residue (side-chain environments are more variable along the side chain, especially for long side chains) and averaging successive temperatures to produce a smoother plot. While this type of compression would yield 124 separate graphs, we present only a limited number of representative plots to illustrate the diversity of behavior that is observed. Plots for several residues, shown in Figure 10, indicate that the temperature dependence of individual Debye–Waller factors can show at least two types of biphasic behavior: one with a small positive slope at low temperature followed by a large positive slope at temperatures greater than 200 K and a second with a small positive slope at both low

Table IV: Difference Distance Matrices

	H1	T1	H2	T2	S1A	H3	T3	S2A	S1B	T4	S1C	S2B	T5	S2C
							320–98 K[a]							
H1	0.01	0.11	0.09	0.02	0.07	0.12	0.40	0.18	0.00	0.10	−0.01	0.16	0.23	0.17
T1		0.02	0.03	0.16	0.20	0.26	0.39	0.38	0.14	0.03	0.05	0.34	0.43	0.37
H2			0.04	0.22	0.09	0.22	0.40	0.29	0.05	0.00	−0.01	0.25	0.35	0.32
T2				0.06	−0.11	0.11	0.13	0.00	−0.10	0.09	−0.07	−0.01	0.11	0.03
S1A					0.04	0.23	0.26	0.24	0.00	−0.02	−0.01	0.18	0.27	0.21
H3						0.02	0.23	0.16	0.13	0.23	0.13	0.13	0.18	0.11
T3							−0.02	0.01	0.14	0.36	0.16	0.04	0.18	0.01
S2A								0.04	0.16	0.25	0.20	0.01	0.01	−0.01
S1B									−0.03	0.00	−0.02	0.10	0.18	0.14
T4										−0.07	−0.05	0.21	0.29	0.28
S1C											−0.01	0.13	0.19	0.18
S2B												−0.03	0.05	−0.03
T5													0.00	0.04
S2C														0.00
av	0.12	0.21	0.17	0.09	0.14	0.16	0.20	0.14	0.09	0.14	0.09	0.12	0.18	0.14
							320–220 K							
H1	0.00	0.13	0.09	0.01	0.05	0.01	0.28	0.10	−0.01	0.06	−0.02	0.06	0.21	0.09
T1		0.02	0.02	0.09	0.16	0.19	0.32	0.31	0.10	−0.02	0.03	0.29	0.39	0.33
H2			0.03	0.14	0.07	0.11	0.35	0.23	0.04	0.00	−0.02	0.20	0.32	0.28
T2				0.04	0.13	0.23	0.19	0.03	−0.08	0.07	−0.08	−0.01	0.15	0.06
S1A					0.04	0.13	0.23	0.19	−0.01	−0.05	−0.02	0.15	0.24	0.18
H3						0.02	0.13	0.11	0.07	0.08	0.06	0.08	0.09	0.04
T3							−0.03	−0.02	0.12	0.29	0.12	0.01	0.11	−0.03
S2A								0.03	0.13	0.17	0.14	0.02	−0.02	−0.04
S1B									−0.03	−0.04	−0.03	0.10	0.16	0.13
T4										−0.02	−0.09	0.12	0.25	0.19
S1C											−0.02	0.11	0.15	0.15
S2B												−0.01	0.01	−0.05
T5													0.03	0.00
S2C														−0.03
av	0.08	0.17	0.14	0.08	0.12	0.01	0.16	0.11	0.08	0.10	0.07	0.09	0.15	0.11

[a] Definitions of secondary structure elements (T, turn; H, helix; S, strand): H1 (residues 3–13); T1 (residues 14–23); H2 (residues 24–34); T2 (residues 35–41); S1A (residues 42–48); H3 (residues 50–60); T3 (residues 61–70); S2A (residues 71–75); S1B (residues 79–86); T4 (residues 87–95); S1C (residues 96–104); S2B (residues 105–110); T5 (residues 111–117); S2C (residues 118–124).

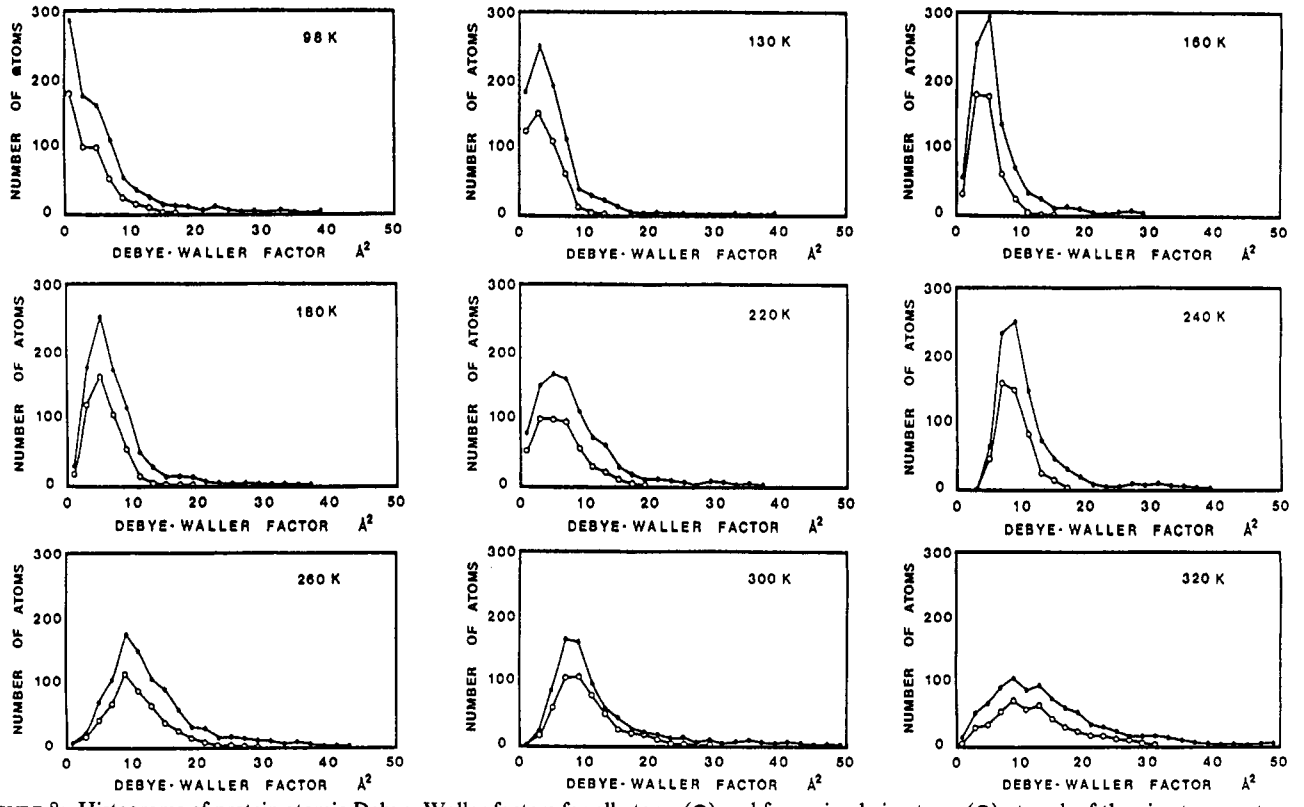

FIGURE 8: Histograms of protein atomic Debye–Waller factors for all atoms (●) and for main-chain atoms (○) at each of the nine temperatures.

and high temperatures with a rapid transition at the intermediate temperature of 200 K. However, certain residues display biphasic behavior, with the break occurring at a substantially different temperature, a modest linear increase with no apparent break in slope, or no change at all with temperature, i.e., zero slope. While both exposed and buried residues

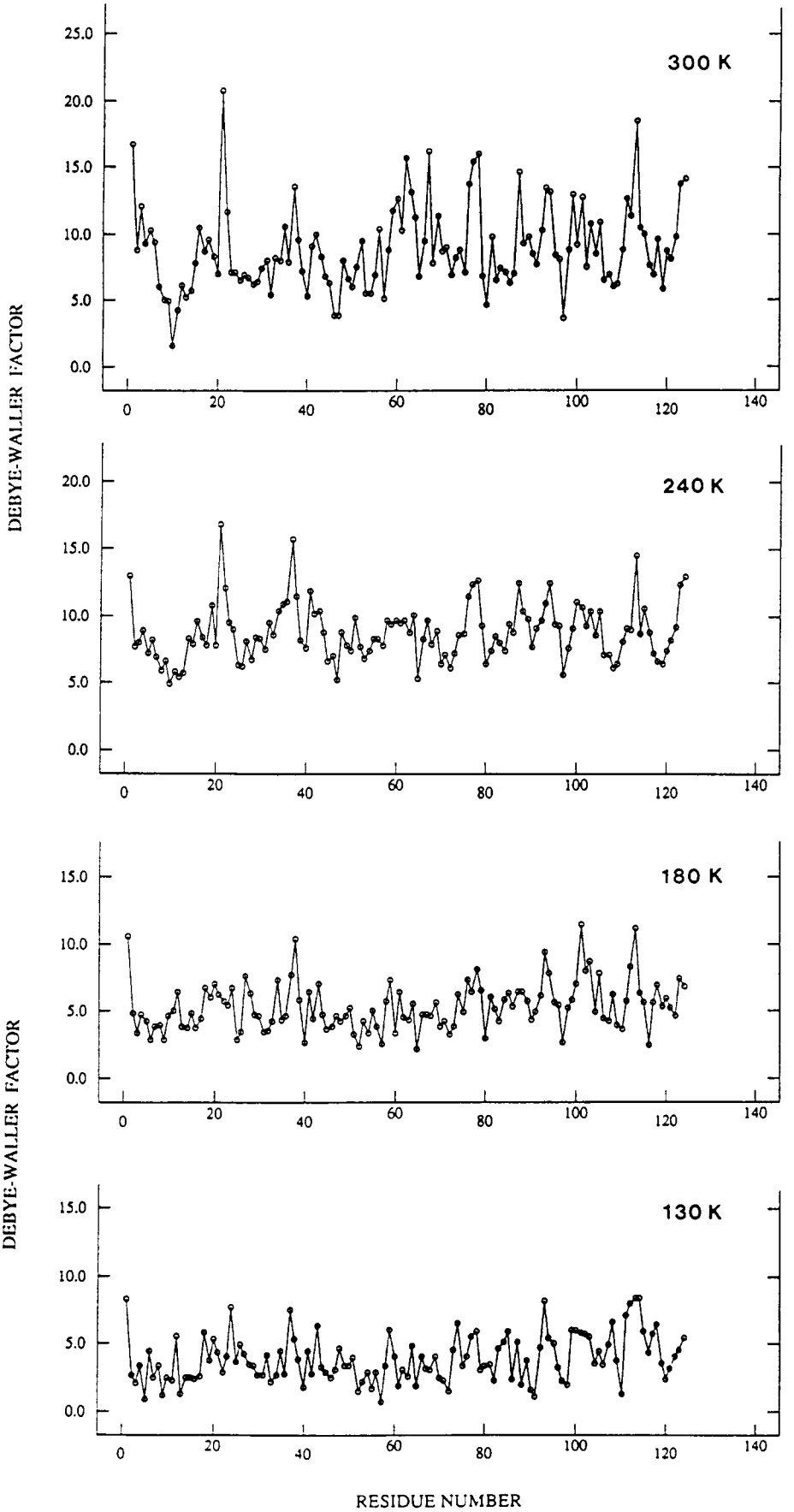

FIGURE 9: Average main-chain (Cα, C, N) Debye–Waller factors as a function of residue number for temperatures of 130, 180, 240, and 300 K. An overall increase as well as a greater range in the Debye–Waller factor profile is observed. Residue 21, the site of proteolytic cleavage in the production of ribonuclease-S, has the largest absolute Debye–Waller factor at elevated temperatures and exhibits the greatest temperature sensitivity.

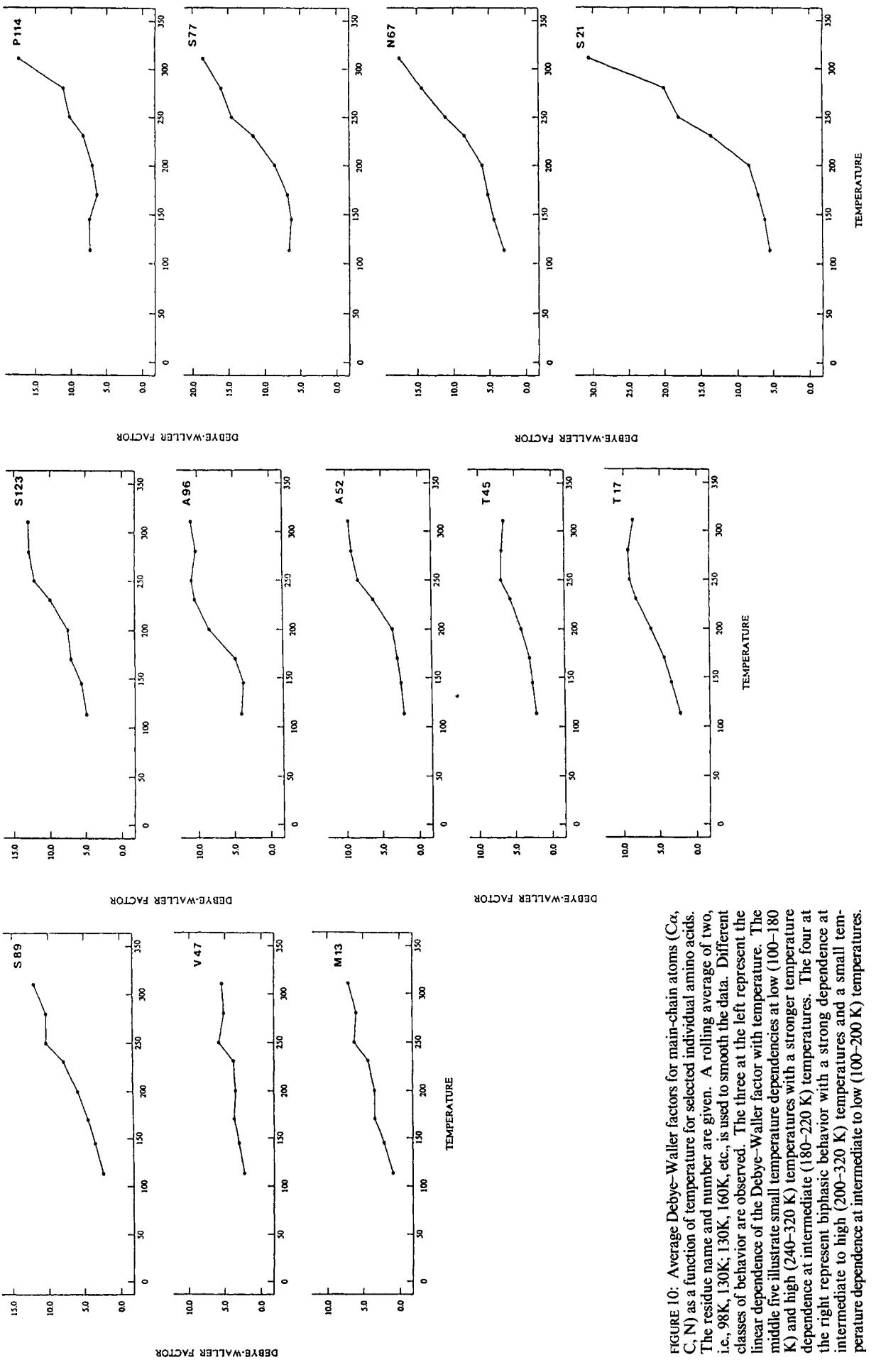

FIGURE 10: Average Debye–Waller factors for main-chain atoms (Cα, C, N) as a function of temperature for selected individual amino acids. The residue name and number are given. A rolling average of two, i.e., 98K, 130K; 130K, 160K, etc., is used to smooth the data. Different classes of behavior are observed. The three at the left represent the linear dependence of the Debye–Waller factor with temperature. The middle five illustrate small temperature dependencies at low (100–180 K) and high (240–320 K) temperatures with a stronger temperature dependence at intermediate (180–220 K) temperatures. The four at the right represent biphasic behavior with a strong dependence at intermediate to high (200–320 K) temperatures and a small temperature dependence at intermediate to low (100–200 K) temperatures.

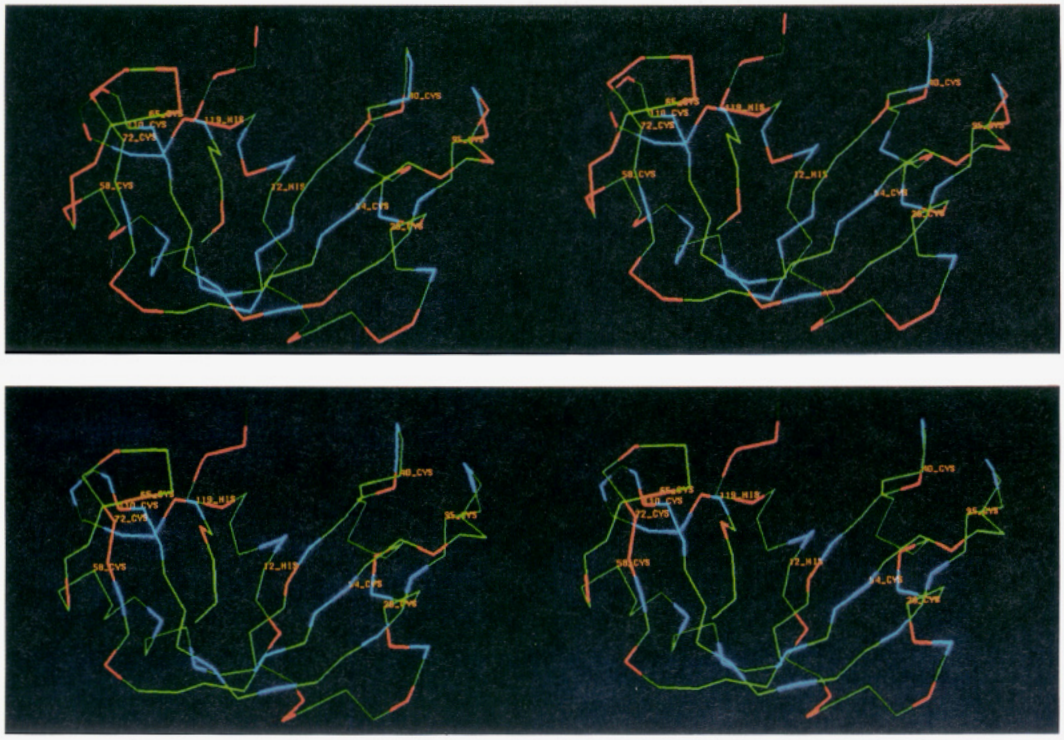

FIGURE 11: Cα structure of ribonuclease-A, in stereo, at 98 K with four disulfide bridges. (a, top) The color coding for absolute changes in the main-chain Debye–Waller factor between 98–130 K average and 300–320 K average is (0–4 Å^2) blue (28 residues), (4–8 Å^2) green (63 residues), and (>8 Å^2) red (33 residues). (b, bottom) The color coding for percentage change in the main-chain Debye–Waller factor between 98–130 K average and 300–320 K average is (<50%) light blue (11 residues), (50–100%) blue (15 residues), (100–250%) green (68 residues), and (>250%) red (30 residues).

exhibit similar types of behavior, side-chain atoms of exposed residues exhibit larger changes in Debye–Waller factors with temperature than side-chain atoms of buried residues. The wide variation in the Debye–Waller behavior for individual amino acids is implicit in the Debye–Waller distributions shown in the histograms of Figure 8.

In the absence of a theoretical model to explain the different types of temperature dependence, it is useful to analyze the percentage change in the Debye–Waller factor over the entire temperature range. Figure 11 maps the percentage and absolute difference in the residue-averaged Debye–Waller factor between 98 and 320 K onto the protein structure. The loops and turns on the exterior surface of the protein clearly exhibit the largest change.

Because mobility is known to correlate with solvent exposure and residue hydrophilicity, it is logical to ask whether changes in mobility are similarly correlated. In fact, little correlation is observed between the percentage change in the Debye–Waller factor and either exposed surface area or residue type. However, a correlation is observed (Figure 12) between the percentage change in the Debye–Waller factor and the average change in the position of individual secondary structure segments computed from the difference distance matrices in Table IV. While T5 (residues 111–117) behaves anomalously, it appears that the link between structural deformation and changes in the Debye–Waller factors is more important than the specific residue type or the amount of solvent-exposed surface area. It is hypothesized that a decreasing Debye–Waller factor leads to a smaller "effective volume" for the atom that leads to, on average, a higher atomic packing density that may contribute to the observed structural deformations.

Discussion

Significance of the Results. As the temperature is increased from 98 to 320 K, the structural and dynamic properties of the protein ribonuclease-A are subtly perturbed. Because the changes are small, it is pertinent to ask whether these perturbations are statistically significant. Random errors have been estimated by standard crystallographic refinement of a number of starting models of the protein sperm whale myoglobin (153 amino acids) against 1.5-Å data (Kuriyan et al., 1987). The results indicate that positional rms uncertainties of 0.1 Å are observed for main-chain atoms while slightly higher uncertainties (0.3 Å) are observed for side-chain atoms. Given the similarity in the number of total atoms, identical resolution limits of 1.5 Å on the diffraction data, and very similar refinement procedures and final R factors, one might expect errors in these ribonuclease-A models to be of the same magnitude. In general, structures solved with data collected at similar temperatures have rms differences of 0.1 Å for main-chain and 0.3–0.4 Å for side-chain atoms while structures solved with data collected at widely separated temperatures have significantly larger deviations (0.3 Å for main-chain and 0.8 Å for side-chain atoms). Moreover, systematic changes observed for both the radius of gyration and probe-accessible volume indicate a linear expansion of the ribonuclease-A molecule with increasing temperature. Random errors in the atomic coordinates would not be expected to produce such changes.

Kuriyan et al. (1987) also estimated the errors in refined Debye–Waller factors to be approximately 15% of their magnitude. Again, the observed changes in the overall and individual Debye–Waller factors in ribonuclease-A over the temperatures examined are generally much larger (138%) than this estimated error. Furthermore, small differences observed between closely spaced data sets tend to be systematic and follow a smooth curve that is physically sensible. Random errors, again, would not be expected to produce this result. We proceed with the premise that the small differences observed in the structure and dynamics of the ribonuclease-A molecule

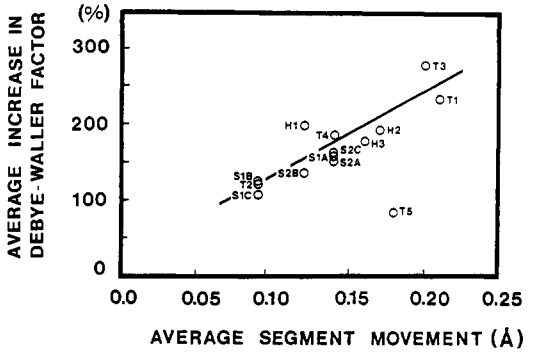

FIGURE 12: Percentage change in the average Debye–Waller factor averaged over residues within secondary structure units (α-helices, strands, turns) versus overall segmental motions for this secondary structure unit (Table IV). There appears to be a correlation between the behavior of the Debye–Waller factor for a secondary structure unit and its ability to change its overall relative position.

with temperature are indeed real and physically meaningful.

The remainder of the discussion will address two questions: (1) Are there different temperature behaviors for different protein molecules? (2) What are some of the contributing factors that are responsible for structure/dynamic changes with temperature?

We observe that raising the temperature produces the following changes in the structural and dynamical properties of the ribonuclease-A molecule: (1) there is a small expansion of 0.4% per 100 K in total protein volume; (2) this expansion is due primarily to movements of the protruding solvent-exposed loops and turns within the protein molecule as well as lower atomic packing densities; (3) the protein atomic Debye–Waller factors have a narrow distribution at low temperature that broadens significantly at higher temperature; (4) the overall Debye–Waller factor behavior is markedly biphasic with the break in slope occurring at approximately 180–200 K; (5) individual amino acid residues within the protein exhibit a wide range of Debye–Waller factor behaviors that include virtual temperature independence, a linear change with temperature, and various types of biphasic behavior; (6) there exists a high correlation between the average movement of secondary structure elements and the average change in the corresponding Debye–Waller factors for that element.

While we cannot draw any conclusions about the general effects of temperature on protein structure, it is believed that protein molecules will have a range of thermal expansion behavior depending on local atomic packing, molecular topology, secondary structure arrangement, and solvent–protein coupling. It is instructive to compare the behavior of ribonuclease-A, a tightly packed, kidney-shaped protein with a central β-sheet and large protruding loops, with the behavior of myoglobin, an oblate spheroidal protein with significant internal cavities resulting from the packing of α-helices about the prosthetic heme group. Ribonuclease-A has a 2–3-fold smaller thermal expansion than myoglobin over an equivalent temperature range. Within the ribonuclease-A molecule, the α-helices undergo larger movements than the individual strands within the β-sheet. Combined with the myoglobin data, this observation would suggest that helical structures are more affected by temperature. For both proteins, thermal expansion occurs chiefly in the larger protruding loops, implying a lower thermal sensitivity for the tightly packed protein core. These observations correlate with ligand-induced conformational changes in proteins, which usually involve movements of helices and exposed loops, and rarely alter the positions of β-sheets. They are also physically sensible: the hydrogen-bonded network in a β-sheet provides a kind of cross-linking that would aid in immobilizing the polypeptide chain. The α-helix, though held relatively rigid internally by hydrogen bonds, generally makes contacts with neighboring secondary structure segments through weaker nonbonded interactions. The results obtained to date for ribonuclease-A and myoglobin show a range of thermal expansion behavior reflecting the highly anisotropic nature of the forces that stabilize protein molecule structure. It would be very interesting to examine the temperature dependence of a β-barrel protein such as β-lactoglobulin.

The other striking result from this study is the demonstration of a temperature-dependent biphasic behavior of the Debye–Waller factor. The continuous change in average Debye–Waller factor with temperature indicates that much of the observed effect can be attributed to molecular motion rather than static disorder and hence is a measure of the dynamic behavior of the protein–water system with temperature. Similar biphasic behavior in other proteins in both crystal and solution states suggests that this phenomenon is a fundamental property of macromolecules in water. However, a caveat that must be mentioned is that the rapid freezing method employed for the low-temperature data sets may cause unsuspected and irrelevant behavior in the cooled protein crystal. It is curious that the unit cell dimensions and protein molecular volumes appear linear over the entire temperature range, with no sign of the discontinuity that is so apparent in the behavior of the Debye–Waller parameter. Furthermore, changes in protein volume account for a small fraction (less than 1%) of the total change in unit cell volume, and large amounts of "bulk" solvent are still unaccounted for. Investigation of these points is planned.

Ribonuclease-A shows an increasingly anharmonic distribution of Debye–Waller factors as the temperature is increased. While the distribution of the Debye–Waller factors suggests more classical behavior below 200 K (Levy et al., 1982; Kuczera et al., 1990; Tilton and Singh, submitted for publication), the steep observed slope in the behavior of the average Debye–Waller factor and the correlated broadening of the Debye–Waller factor distribution above 200 K suggest increasingly anharmonic dynamics. Large anharmonic motions probably involve groups of bonded or nonbonded atoms moving collectively, while harmonic behavior is more likely to involve individual atomic vibrations or motions of smaller ensembles. Around 200 K, a change takes place in the protein–solvent system such that large motions become more favorable as the temperature is increased. This effect seems to occur over most of the protein at nearly the same temperature, despite the marked differences in molecular structure and local environments of individual residues. Such a global property leads one to suspect that a change in the structure and/or dynamics of the free and bound solvent is responsible. To determine whether the bulk solvent in the crystal interstices or the "bound" solvent layer directly interacting with the protein is involved, one could carry out a similar crystallographic study with temperature on proteins with widely different solvent contents and lattice channel arrangements. Crambin (Teeter & Hope, 1986) or triclinic lysozyme (Muchmore & Watenpaugh, 1989) would appear to be excellent candidates for the lower boundary of solvent content while lysozyme in different space groups and with different unit cell dimensions would permit an investigation of the role of crystal contacts and lattice effects on the dependence of protein structure and dynamics with temperature. In the meantime, these ribonuclease-A structures should provide data to help further studies of the bound solvent as a function of temperature and, when analyzed in detail, may help to reveal a deeper understanding of the

coupling between solvent and protein atoms.

ACKNOWLEDGMENTS

We thank Steve Burley, Robert Campbell, William Gilbert, Irwin Kuntz, John Kuriyan, and Kieth Watenpaugh for stimulating discussions and unpublished data.

Registry No. Ribonuclease A, 9001-99-4.

REFERENCES

Avey, H. P., Boles, M. O., Carlisle, C. H., Evans, S. A., Morris, S. J., Palmer, R. A., Woolhouse, B. A., & Shall, S. (1967) *Nature (London) 213*, 556–557.

Bauminger, E. R., Cohen, S. G., Nowik, I., Ofer, S., & Yariv, J. (1983) *Proc. Natl. Acad. Sci. U.S.A. 80*, 736–740.

Borkakoti, N. (1983) *Eur. J. Biochem. 132*, 89–94.

Borkakoti, N., Moss, D. S., & Palmer, R. A. (1982) *Acta Crystallogr. B38*, 2210–2217.

Borkakoti, N., Moss, D. S., Stanford, M. J., & Palmer, R. A. (1984) *J. Crystallogr. Spectrosc. Res. 14*, 467–494.

Campbell, R. L., & Petsko, G. A. (1987) *Biochemistry 26*, 8579–8584.

Connolly, M. L. (1985) *J. Am. Chem. Soc. 107*, 1118–1124.

Cusack, S. (1989) in *The Enzyme Catalysis Process: Energetics, Mechanism and Dynamics* (Cooper, A., Houben, J., & Chien, L., Eds.) pp 103–122, Plenum Press, New York and London.

Dewan, J. C., & Tilton, R. F., Jr. (1987) *J. Appl. Crystallogr. 20*, 130–132.

Doster, W., Bachleitner, A., Dunau, R., Hiebl, M., & Luscher, E. (1986) *Biophys. J. 50*, 213–219.

Doster, W., Cusack, S., & Petry, W. (1989) *Nature (London) 337*, 754–756.

Douzou, P. (1977) *Cryobiochemistry: An Introduction*, Academic Press, New York.

Frauenfelder, H., Petsko, G. A., & Tsernoglou, D. (1979) *Nature (London) 280*, 558.

Frauenfelder, H., Hartmann, H., Karplus, M., Kuntz, I. D., Jr., Kuriyan, J., Parak, F., Petsko, G. A., Ringe, D., Tilton, R. F., Jr., Connolly, M. L., & Max, N. (1987) *Biochemistry 26*, 254–261.

Gilbert, W. A., Lord, R. C., Petsko, G. A., & Thamann, T. J. (1982) *J. Raman Spectrosc. 12*, 173–179.

Hartmann, H., Parak, F., Steigemann, W., Petsko, G. A., Ringe-Ponzi, D., & Frauenfelder, H. (1982) *Proc. Natl. Acad. Sci. U.S.A. 79*, 4967–4971.

Hass, D. J., & Rossmann, M. G. (1970) *Acta Crystallogr. B26*, 998–1004.

Hope, H. (1988) *Acta Crystallogr. B44*, 22–26.

Hope, H. (1990) *Annu. Rev. Biophys. Biophys. Chem. 19*, 107–126.

Hope, H., & Power, P. P. (1983) *J. Am. Chem. Soc. 105*, 5320–5324.

Hope, H., Frolow, F., van Bohlen, K., Makowski, I., Kratky, C., Halfon, Y., Danz, H., Webster, P., Bartels, K. S., Wittmann, H. G., & Yonath, A. (1989) *Acta Crystallogr. B45*, 190–199.

Huffman, J. C., Moody, D. C., Rathke, J. W., & Schaeffer, R. (1973) *J. Chem. Soc., Chem. Commun.*, 308.

Jones, T. A. (1982) in *Computational Crystallography* (Sayre, D., Ed.) pp 303–317, Oxford University Press, New York.

Kartha, G., Bello, J., & Harker, D. (1967) *Nature (London) 213*, 862–865.

Keller, H., & Debrunner, P. G. (1980) *Phys. Rev. Lett. 45*, 68–71.

King, M. V., Magdoff, B. S., Adelman, M. B., & Harker, D. (1956) *Acta Crystallogr. 9*, 460–465.

Konnert, J. H., & Hendrickson, W. A. (1980) *Acta Crystallogr. A36*, 344–349.

Kuczera, K., Kuriyan, J., & Karplus, M. (1990) *J. Mol. Biol. 213*, 351–373.

Kuriyan, J., Karplus, M., & Petsko, G. A. (1987) *Proteins: Struct., Funct., Genet. 2*, 1–12.

Levy, R. M., Perahia, D., & Karplus, M. (1982) *Proc. Natl. Acad. Sci. U.S.A. 79*, 1346–1350.

Listemann, M. L., Dewan, J. C., & Schrock, R. R. (1985) *J. Am. Chem. Soc. 107*, 7207–7208.

McPherson, A., Brayer, G., & Morrison, R. (1986) *Biophys. J. 49*, 209–219.

Muchmore, S. W., & Watenpaugh, K. D. (1988) *Proc. Am. Crystallogr. Assoc. Meet., Philadelphia*, Abstract L2, 43.

Muchmore, S. W., & Watenpaugh, K. D. (1989) *Proc. Am. Crystallogr. Assoc. Meet., Seattle*, Abstract HB3, 43.

Nishikawa, K., Ooi, T., Isogai, Y., & Saito, N. (1972) *J. Phys. Soc. (Jpn.) 32*, 1331–1337.

North, A. C. T., Phillips, D. C., & Mathews, F. S. (1968) *Acta Crystallogr. A24*, 351–359.

Parak, F., Knappk, E. W., & Kucheida, D. (1982) *J. Mol. Biol. 161*, 177–194.

Parak, F., Hartmann, H., Aumann, K. D., Reuscher, H., Rennekamp, G., Bartunik, H., & Steigemann, W. (1987) *Eur. Biophys. J. 15*, 237–249.

Pederson, S. F., Dewan, J. C., Eckman, R. R., & Sharpless, K. B. (1987) *J. Am. Chem. Soc. 109*, 1279–1282.

Peterson-Kennedy, S. E., McGourty, J. L., Kalweit, J. A., & Hoffman, B. M. (1986) *J. Am. Chem. Soc. 108*, 1739–1746.

Petsko, G. A. (1975) *J. Mol. Biol. 96*, 381–392.

Petsko, G. A., & Ringe, D. (1984) *Annu. Rev. Biophys. Bioeng. 13*, 331–371.

Schumann, H., Albrecht, I., Loebel, J., Hahn, E., Hossain, M. B., & van der Helm, D. (1986) *Organometallics 5*, 1296–1304.

Stout, G. H., & Jensen, L. H. (1989) in *X-ray Structure Determination—A Practical Guide*, 2nd ed., John Wiley and Sons, New York.

Svensson, L. A., Sjolin, L., Gilliland, G. L., Finzel, B. C., & Wlodawer, A. (1986) *Proteins: Struct., Funct., Genet. 1*, 370–375.

Teeter, M. M., & Hope, H. (1986) *Ann. N.Y. Acad. Sci. 482*, 163–165.

Usha, M. G., & Wittebort, R. J. (1989) *J. Mol. Biol. 208*, 669–678.

Wlodawer, A., & Sjolin, L. (1983) *Biochemistry 22*, 2720–2728.

Wlodawer, A., Borkakoti, N., Moss, D. S., & Howlin, B. (1986) *Acta Crystallogr. B42*, 379–387.

Wlodawer, A., Svensson, L. A., Sjolin, L., & Gilliland, G. (1988) *Biochemistry 27*, 2705–2717.

Wyckoff, H. W., Doscher, M., Tsernoglou, D., Inagami, T., Johnson, L. N., Hardman, K. D., Allewell, N. M., Kelly, D. M., & Richards, F. M. (1967) *J. Mol. Biol. 27*, 563–578.

Young, A. C. M., Dewan, J. C., Thompson, A. W., & Nave, C. (1990) *J. Appl. Crystallogr. 23*, 215–218.